



Hypothalamic growth hormone receptor (GHR) controls hepatic glucose production in nutrient-sensing leptin receptor (LepRb) expressing neurons

Gillian Cady^{1,7}, Taylor Landeryou¹, Michael Garratt¹, John J. Kopchick², Nathan Qi³, David Garcia-Galiano⁴, Carol F. Elias⁴, Martin G. Myers Jr.³, Richard A. Miller¹, Darleen A. Sandoval⁵, Marianna Sadagurski^{6,*,7}

ABSTRACT

Objective: The GH/IGF-1 axis has important roles in growth and metabolism. GH and GH receptor (GHR) are active in the central nervous system (CNS) and are crucial in regulating several aspects of metabolism. In the hypothalamus, there is a high abundance of GH-responsive cells, but the role of GH signaling in hypothalamic neurons is unknown. Previous work has demonstrated that the *Ghr* gene is highly expressed in LepRb neurons. Given that leptin is a key regulator of energy balance by acting on leptin receptor (LepRb)-expressing neurons, we tested the hypothesis that LepRb neurons represent an important site for GHR signaling to control body homeostasis.

Methods: To determine the importance of GHR signaling in LepRb neurons, we utilized Cre/loxP technology to ablate GHR expression in LepRb neurons (LepR^{EYFPΔGHR}). The mice were generated by crossing the LepR^{cre} on the cre-inducible ROSA26-EYFP mice to GHR^{L/L} mice. Parameters of body composition and glucose homeostasis were evaluated.

Results: Our results demonstrate that the sites with GHR and LepRb co-expression include ARH, DMH, and LHA neurons. Leptin action was not altered in LepR^{EYFPΔGHR} mice; however, GH-induced pStat5-IR in LepRb neurons was significantly reduced in these mice. Serum IGF-1 and GH levels were unaltered, and we found no evidence that GHR signaling regulates food intake and body weight in LepRb neurons. In contrast, diminished GHR signaling in LepRb neurons impaired hepatic insulin sensitivity and peripheral lipid metabolism. This was paralleled with a failure to suppress expression of the gluconeogenic genes and impaired hepatic insulin signaling in LepR^{EYFPΔGHR} mice.

Conclusion: These findings suggest the existence of GHR-leptin neurocircuitry that plays an important role in the GHR-mediated regulation of glucose metabolism irrespective of feeding.

© 2017 The Authors. Published by Elsevier GmbH. This is an open access article under the CC BY-NC-ND license (<http://creativecommons.org/licenses/by-nc-nd/4.0/>).

Keywords Growth hormone receptor; Hypothalamus; Leptin receptor; Glucose production; Liver

1. INTRODUCTION

Growth hormone (GH) signaling plays a major role in regulating body composition and glucose metabolism [1]. Increased protein accretion in muscle and lipolysis in adipose tissue are biological consequences of GH action and together promote a lean phenotype [2]. Despite its ability to improve body composition, GH has also been described as a diabetogenic agent with the ability to increase hepatic glucose production [3]. Nevertheless, clinical trials using GH therapy to treat

patients with obesity and type 2 diabetes demonstrated improvements in body composition, glucose tolerance, and insulin sensitivity [4,5]. In both human and mouse brain, GH and the GH receptor (GHR) are present in regions known to participate in the regulation of feeding behavior, energy balance, and glucose metabolism such as the hypothalamus, hippocampus, and amygdala [6–10]. Upon GHR activation, the signal transducer and activator of transcription 5 (Stat5) is recruited and regulates the transcription of genes directly controlled by GH [11,12]. In the arcuate nucleus of the hypothalamus (ARH), GHR is involved in the

¹Department of Pathology and Geriatrics Center, University of Michigan Medical School, USA ²Edison Biotechnology Institute, Ohio University, Athens, OH, USA ³Division of Metabolism, Endocrinology and Diabetes, Department of Internal Medicine, University of Michigan Medical School, Ann Arbor, MI, USA ⁴Department of Molecular and Integrative Physiology, University of Michigan Medical School, Ann Arbor, MI, USA ⁵Department of Surgery, University of Michigan Medical School, Ann Arbor, MI, USA ⁶Division of Geriatric and Palliative Medicine, Department of Internal Medicine, University of Michigan Medical School, Ann Arbor, MI, USA

⁷ Current address: Department of Biological Sciences, Integrative Biosciences Center (IBio), Wayne State University, Detroit, MI, USA.

*Corresponding author. Department of Biological Sciences, Integrative Biosciences Center, Wayne State University, Room 2418 IBio, 6135 Woodward, Detroit, MI 48202, USA. E-mail: sadagurski@wayne.edu (M. Sadagurski).

Abbreviations: CNS, central nervous system; GH, growth hormone; GHR, growth hormone receptor; LepR, leptin receptor; Stat3, signal transducer and activator of transcription 3; Stat5, signal transducer and activator of transcription 5; POMC, proopiomelanocortin; ARH, arcuate nucleus of the hypothalamus; DMH, dorsomedial hypothalamic nucleus; LHA, lateral hypothalamus; PVH, paraventricular hypothalamic nucleus

Received February 15, 2017 • Revision received February 28, 2017 • Accepted March 4, 2017 • Available online 16 March 2017

<http://dx.doi.org/10.1016/j.molmet.2017.03.001>

negative feedback loops that regulate GH production and secretion from somatotrophs of the pituitary [7]. Systemic administration of GH induces expression of the *c-fos* gene, a marker of neuronal activity, on the hypothalamic neuropeptide Y (NPY) and somatostatin neurons [13]. The majority of NPY mRNA-containing cells in the ARH express the GHR gene, suggesting that NPY neurons in the ARH mediate the feedback effect of GH on the hypothalamus. Feedback inhibition of GH production is predicated upon proper function of the GHR signaling cascade [14]. Long-lived GH receptor (GHR) knockout mice ($GHR^{-/-}$) are obese, with elevated leptin levels and increased insulin sensitivity [15]. Deletion of hypothalamic GH-releasing hormone (GHRH) leads to isolated GH deficiency and increases lifespan, while overexpression of GH in the CNS results in hyperphagia-induced obesity, highlighting the importance of GH signals in hypothalamic neurons [16,17]. In contrast, mice with modest increases in GH levels show improvements in glucose homeostasis with minimum effects on adiposity [18]. We recently reported that $GHR^{-/-}$ mice have reduced formation of both orexigenic and anorexigenic hypothalamic projections, while disruption of GHR specifically in liver, a mutation that reduces circulating IGF1, had no effect on hypothalamic development [19]. While some suggest that CNS effects of GH signaling are indirect, via increases in circulating IGF1 [20], these data show that GHR has a direct effect on the CNS; however, the precise role of GHR in hypothalamic neurons remains largely unknown. Nutrient sensing, leptin receptor expressing (LepRb) neurons sense and integrate signals relevant to nutrient homeostasis to control energy balance and metabolism [21]. Previous studies also indicate that leptin can modulate GH secretion and the GH response to GHRH [22]. LepRb neurons are widely distributed within the hypothalamic ARH, VMH, DMH, LHA, and some additional sites that also express GHR [10,23]. Recent transcriptome analysis of LepRb expressing neurons revealed that the *Ghr* gene is strongly enriched in LepRb neurons [24]. Given the crucial role of LepRb neurons in the regulation of energy and glucose metabolism, along with potential overlap between LepRb and GH-responsive cells, we hypothesized that LepRb neurons represent an important site for GH signaling to control metabolism. We therefore deleted GHR specifically in LepRb neurons and examined parameters of energy homeostasis and glucose metabolism in these mice.

2. MATERIALS AND METHODS

2.1. Animals

$GHR^{L/L}$ and $LepR^{cre}$ mice on the ROSA26 background were described previously [21,25]. Mice were bred in our colony at the University of Michigan. Procedures involved in this study were approved by the University of Michigan Committee on the Use and Care of Animals (IACUC). Animals were fed breeder chow diet containing 5 kcal %fat or high fat diet containing 45 kcal %fat (Research Diets, Inc). Most of the presented data relates to male mice, unless otherwise stated.

2.2. Metabolic analysis

Lean and fat body mass were assessed by a Bruker Minispec LF 90II NMR-based device. Blood glucose levels were measured on random-fed or overnight-fasted animals in mouse-tail blood using Glucometer Elite (Bayer). Intraperitoneal glucose tolerance tests were performed on mice fasted for 16 h overnight. Animals were then injected intraperitoneally with D -glucose (2 g/kg), and blood glucose levels were measured as before [26]. For an insulin tolerance test, animals fasted for 5 h received an intraperitoneal injection of human insulin (0.5 units/kg; Novo Nordisk). Blood insulin and leptin levels were determined on serum from tail vein bleeds using a Rat Insulin ELISA kit and Mouse Leptin ELISA kit (Crystal Chem. Inc.). For food intake measurements

mice were singly housed and food intake was measured for 6 consecutive days. Plasma Triglycerides, Low Density Lipoprotein (LDL) and Free Fatty Acids were assessed using spectrophotometric assay kits purchased from Wako Diagnostics (Richmond, VA).

For peripheral leptin stimulation, mice were treated with either 5 mg/kg recombinant mouse leptin (provided by Dr. A Parlow, National Hormone and Pituitary Program, Torrance, CA) or vehicle, injected i.p. and perfused 2 h later. For peripheral GH stimulation (12.5 μ g/100 g BW, GroPep Bioreagents Pty Ltd, Australia), mice were injected i.p. and perfused 1.5 h later.

2.3. Western blotting

Male mice were fasted overnight (18 h). For insulin stimulation, human insulin (5 U) was injected through the inferior vena cava. Liver was dissected and immediately frozen in liquid nitrogen after 5 min of insulin stimulation. For immunoprecipitation, liver extracts were incubated with rabbit polyclonal antibodies against Irs1 for 3 h at 4 °C on a rocker. Then protein A-Sepharose was added and incubated for 1 h at 4 °C. Phosphorylated or total protein was analyzed by immunoblotting with specific antibodies against Irs1 and phosphotyrosine (Millipore). Phosphorylated or total Akt were analyzed by immunoblotting with specific antibodies (Cell Signaling Technology).

2.4. Hyperinsulinemic-euglycemic clamp

At 14 weeks of age, the right jugular vein and carotid artery were surgically catheterized, and male mice were given 5 days to recover from the surgery. After 5–6 h fast, hyperinsulinemic-euglycemic clamp studies were performed on unrestrained, conscious mice by the University of Michigan Animal Phenotyping Core using the protocol adopted from the Vanderbilt Mouse Metabolic Phenotyping Center [27], consisting of a 90-min equilibration period followed by a 120-min experimental period ($t = 0$ –120 min). Insulin was infused at 2.5 mU/kg/min. To estimate insulin-stimulated glucose uptake in individual tissues, a bolus injection of 2-[1-14C]deoxyglucose (PerkinElmer Life Sciences) (10 μ Ci) was given at $t = 78$ min while continuously maintaining the hyperinsulinemic-euglycemic steady state. At the end of the experiment, animals were anesthetized with an intravenous infusion of sodium pentobarbital, and tissues were collected and immediately frozen in liquid nitrogen for later analysis of tissue 14C radioactivity. Plasma insulin was measured using the Millipore rat/mouse insulin ELISA kits. For determination of plasma radioactivity of [3-3H]-glucose and 2-[1-14C] deoxyglucose, plasma samples were deproteinized and counted using a liquid scintillation counter. For analysis of tissue 2-[1-14C] deoxyglucose 6-phosphate, tissues were homogenized in 0.5% perchloric acid, and the supernatants were neutralized with KOH. Aliquots of the neutralized supernatant with and without deproteinization were counted for determination of the content of 2-[1-14C] deoxyglucose phosphate.

2.5. RNA extraction and qPCR

Hypothalami were carefully dissected using Brain Matrices (Baintree Scientific, Braintree, MA). Isolated mRNA from this tissue was analyzed using quantitative real-time PCR. RNA was isolated using the QIAGEN RNeasy Kit (QIAGEN, Valencia, CA), which was combined with the RNase-Free DNase Set (QIAGEN, Valencia, CA). Total RNA was extracted from tissues with Trizol (Gibco BRL) and reverse transcribed using iscript cDNA kit (Bio-Rad Laboratories Inc.). Relative expression of target mRNAs was adjusted for total RNA content by beta-actin RNA quantitative PCR. Quantitative PCR was performed on an ABI-PRISM 7900 HT Sequence Detection system (Applied Biosystems, Foster City, CA). Each reaction was carried out in triplicate as previously

described [28]. Primers used including the following: *AgRP* F: AGGGCA TCAGAAGCCTGACCA, *AgRP* R: CTTGAAGAAGCGGCAGTAGCAC, *POMC* F: AAGAGCAGTGACTAAGAGAGGCCA, *POMC* R: ACATCTATGGAGGTCT-GAAGCAGG, *NPY* F: TAGGTAACAAACGAATGG GG, *NPY* R: AGG ATGA-GATGAGATGTGGG, *LepRb* R: GGAGACAGAGGCCAGACATT, *LepRb* F: AACTTCCTCCAGTCCAAAAG-3, *GHR* R: GCGCTGAACTGGACCC TGCTGAAT, *GHR* F: GGGGGTCTGGACTGGGGAGCTG, *IGF-1* R: TCGCATCTCTTCTATCTGGCCCTGT, *IGF-1* F: CGAGTACATCTCCAGCCTCT CAGA, *G6Pc* F: GGCTCACTTCCCATCAGG, *G6Pc* R: ATCCAAGTGC-GAAACCAAACAG, *Pck1* F: CCCACTGGGAACACAAACTT, *Pck1* R: CCTTCTTCTCTTTGGATGATCT.

2.6. Perfusion and histology

Male mice were anesthetized (IP) with avertin and transcardially perfused with phosphate-buffered saline (PBS) (pH 7.5) followed by 4% paraformaldehyde (PFA). Brains were post-fixed, sank in 30% sucrose, frozen in OCT medium, and then sectioned coronally (30 μ m) using a Leica 3050S cryostat. Six series were collected and stored at -20°C in cryoprotectant, until processed for immunohistochemistry as previously described [19,29]. For immunohistochemistry, free-floating brain sections were washed in PBS, blocked using 3% normal donkey serum (NDS) and .3% Triton X-100 in PBS and then stained with primary overnight in blocking buffer. For pStat3 and pStat5 immunostaining, sections were pretreated for 20 min in 0.5% NaOH and 0.5% H_2O_2 in potassium PBS, followed by immersion in 0.3% glycine for 10 min. Sections were then placed in 0.03% SDS for 10 min and placed in 4% normal serum plus 0.4% Triton X-100 plus 1% BSA for 20 min before incubation for 24 h with a rabbit anti-pStat3 antibody (1:1000; Cell Signaling Technology, Danvers, MA) or a rabbit anti-pStat5 antibody (1:1000; Cell Signaling Technology, Danvers, MA). Sections were mounted onto Superfrost Plus slides (Fisher Scientific, Hudson, NH) and cover slips added with ProLong Antifade mounting medium (Invitrogen, Carlsbad, CA). Microscopic images were obtained using an Olympus Fluoview 500 Laser Scanning Confocal Microscope (Olympus, Center Valley, PA) equipped with a 20 \times objective.

2.7. Double-label in situ hybridization/immunohistochemistry

Double-label ISH and immunohistochemistry (IHC) was performed as previously described [30,31]. Briefly, free-floating sections from control and deleted mice ($n = 3/\text{group}$) were rinsed in DEPC-treated PBS and treated with 0.1% sodium borohydride for 15 min. Sections were treated with 0.25% acetic anhydride in 0.1 M triethanolamine (TEA, pH 8.0) for 10 min then washed in $2 \times \text{SSC}$. The GHR riboprobe (847 bp of size) was generated from ARH cDNA using T3 CAGAGATGCAATTAACCCCT CAC-TAAAGGGAGACCAAGTGTCTGCCCTGAA and T7 CCAAGCCTT CTAA-TACGACTCACTATAGGGAGACTTTGGAAGTGGGACTGGGG primers. The ^{35}S -labeled GHR riboprobe was diluted to 10^6 cpm/mL in a hybridization solution containing 50% formamide, 10 mM Tris-HCl (pH 8.0), 5 mg tRNA (Invitrogen), 10 mM dithiothreitol (DTT), 10% dextran sulfate, 0.3 M NaCl, 1 mM EDTA, and $1 \times$ Denhardt's solution. The sections were incubated overnight at 50°C in the hybridization solution containing the riboprobe. Subsequently, sections were treated with RNase A, submitted to stringency washes in SSC, and incubated in anti-GFP (1:5,000; Aves Labs) overnight at room temperature. The next day, sections were incubated for 1.5 h in secondary antibody (biotin-conjugated donkey anti-chicken, 1:1,000, Jackson Labs) and for 1 h in biotin-avidin complex (1:500, Vector Labs). Peroxidase reaction was performed using 3, 3'-diaminobenzidine tetrahydrochloride (DAB; Sigma) as chromogen, and sections were mounted onto SuperFrost plus slides and dried overnight at room temperature. Tissue was dehydrated in increasing concentrations of ethanol and slides were placed in X-ray film

cassettes with BMR-2 film (Kodak) for 2 days and then dipped in NTB-2 autoradiographic emulsion (Kodak), dried, and stored in light-protected boxes at 4°C for 2 weeks. Finally, slides were developed with D-19 developer (Kodak), dehydrated in graded ethanol, cleared in xylenes, and coverslipped with Permaslip.

2.8. Images and data analysis

All sections used for ISH/IHC were visualized with a Zeiss M2 microscope. Photomicrographs were produced by capturing images with a digital camera (Axiocam, Zeiss) mounted directly on the microscope using the Zen software. Cells were considered dual labeled if the density of silver grains overlying the cytoplasm (GFP-IR) of the cell was at least $3 \times$ greater than the background level. Only one representative section and one side of the brain was counted per mouse per group; therefore, no correction for double counting was used. Adobe Photoshop CS6 image-editing software was used to integrate photomicrographs into plates. Only sharpness, contrast and brightness were adjusted.

2.9. Statistical analysis

Unless otherwise stated, mean values \pm SEM are presented in graphics, and significance was determined by a Student's *t*-test. A *p*-value less than 0.05 was considered statistically significant.

3. RESULTS

3.1. Generation of *LepR^{EYFPΔGHR}*-mice

To inactivate GHR specifically in leptin receptor expressing neurons (*LepRb*), we crossed *LepR^{cre}* on the cre-inducible ROSA26-EYFP background together with *GHR^{fl}* mice, in which the GHR coding sequence was surrounded by LoxP sites [21]. *LepR^{EYFPΔGHR}*-mice are born at the expected Mendelian ratio and are of normal size and appearance. To determine the potential neuronal groups where GHR and *LepRb* converge, we performed dual in situ hybridization (ISH) for GHR and immunohistochemistry (IHC) for GFP on the same coronal brain sections of *LepRb^{EYFP}* and *LepR^{EYFPΔGHR}*-mice. The *LepRb* neurons were revealed by the expression of GFP. The percentage of dual-labeled cells for both GFP-IR and GHR mRNA expression in *LepRb^{EYFP}* and *LepR^{EYFPΔGHR}* include ARH, DMH and LHA neurons (Figure 1A, B and Suppl. Figure 1A).

Consistent with restricted inactivation of the GHR in defined subpopulations of *LepRb* hypothalamic neurons, qPCR analysis revealed no alterations in overall hypothalamic GHR gene expression (Figure 1C). Similarly, GHR expression in peripheral tissues including liver, muscle, pancreas, and pituitary remained unchanged in *LepR^{EYFPΔGHR}*-mice (Figure 1C).

Furthermore, serum IGF-1 and GH levels were not significantly different between *LepR^{EYFPΔGHR}* and controls (Suppl. Figure 1B, C), and IGF1 mRNA levels in liver were similar in *LepR^{EYFPΔGHR}* and control mice (Figure 1D).

GH has been shown to activate several intracellular signaling pathways, including the JAK/Stat5 pathway [32,33]. Cells that exhibit pStat5-immunoreactivity after an acute GH stimulus are considered to be GH responsive [11]. We next determined the functional effects of *LepRb* neuron-restricted GHR deficiency on GH ability to activate the Stat5 pathway in control *LepR^{EYFP}* and *LepR^{EYFPΔGHR}*-mice. In the basal state, about 10% of the ARH *LepRb* neurons contained immunoreactive pStat5 in fasted control and *LepR^{EYFPΔGHR}*-mice (Figure 2). Acute intraperitoneal GH treatment significantly induced pStat5 in control mice. By contrast, GH treatment of *LepR^{EYFPΔGHR}* mice showed a significantly lower percentage of ARH *LepRb* neurons containing pStat5-IR cells (Figure 2). As a measure of *LepRb* signaling [21], we

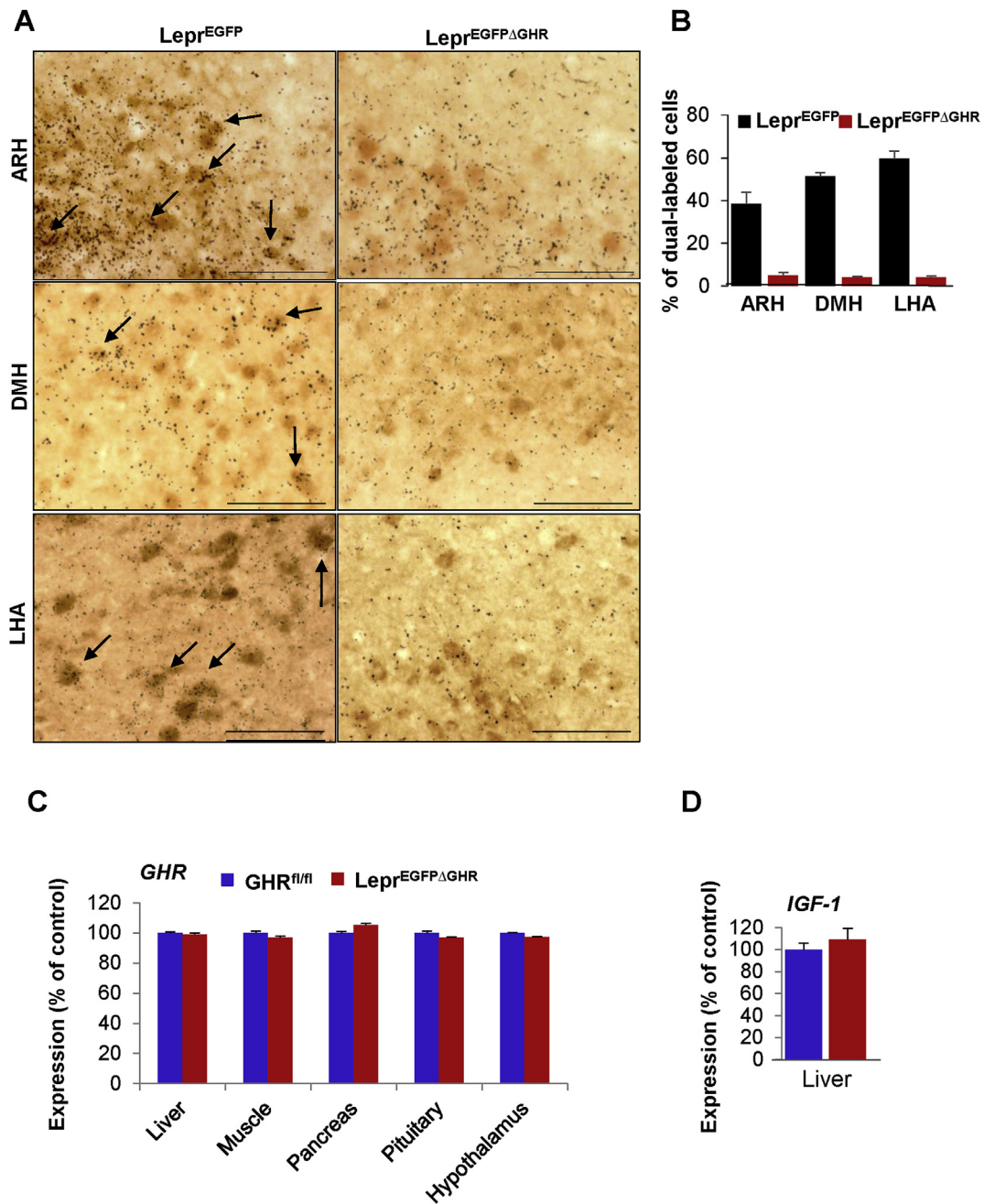


Figure 1: Generation and validation of $Lepr^{EYFP\Delta GHR}$ -mice. (A) Dual-label histochemistry was performed on coronal sections of mouse brains. Neurons with GFP-IR, which reports on LepRb expression, are stained brown. Neurons expressing GHR mRNA have overlying punctate black silver granules. Strong co-expression of LepRb and GHR was observed in the hypothalamic ARH, DMH, and LHA (examples indicated by arrows). Co-expression in other regions of the hypothalamus was minimal. Scale bar = 50 μ m. (B) Bar graph shows percent of dual-labeled cells in the ARH, DMH, and LHA in 7-week-old $Lepr^{EGFP}$ and $Lepr^{EYFP\Delta GHR}$ -mice. (C) *GHR* gene expression in liver, muscle, pancreas, pituitary, and whole hypothalamus and (D) *IGF-1* gene expression in 7-week-old $GHR^{fl/fl}$ and $Lepr^{EYFP\Delta GHR}$ -mice. See also Figure S1A.

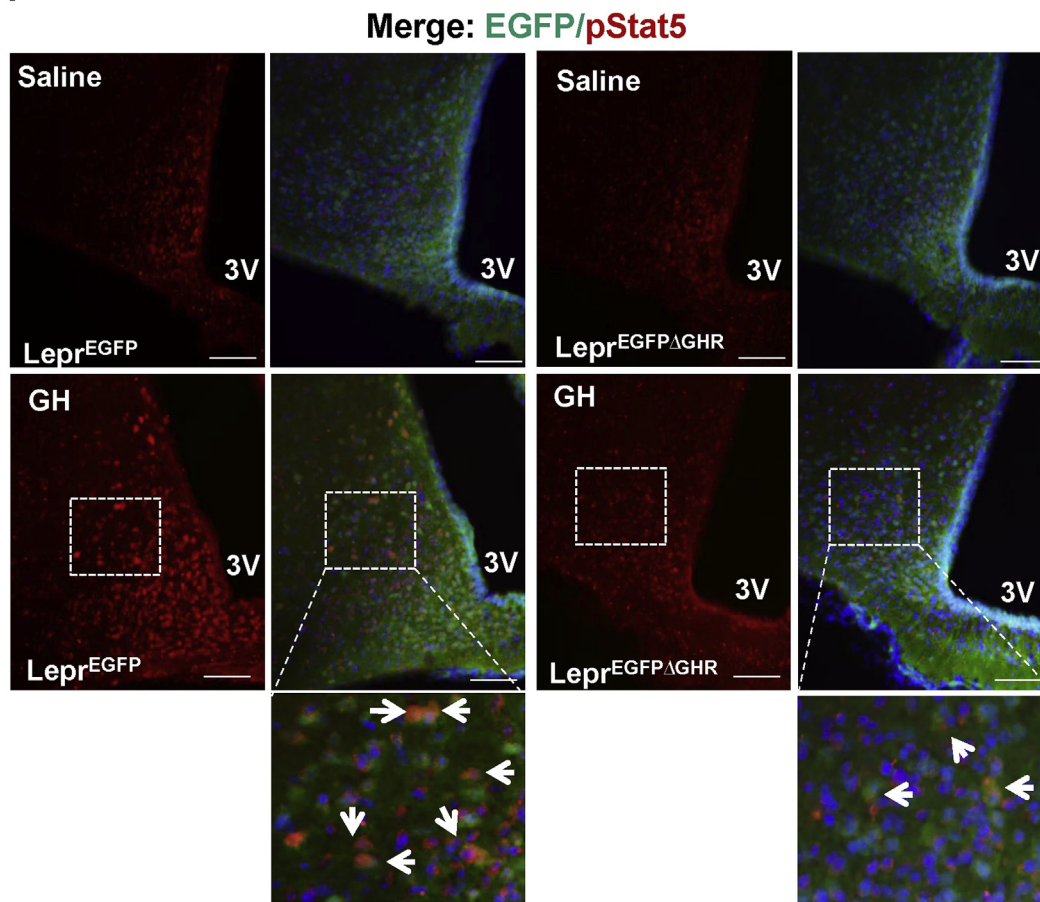
measured leptin-stimulated accumulation of pStat3 in the hypothalamus of $Lepr^{EYFP\Delta GHR}$ -mice. We found that acute leptin treatment promotes similar levels of hypothalamic pStat3 in control and $Lepr^{EYFP\Delta GHR}$ mice; demonstrating that LepRb-Stat3 signaling was not impaired in $Lepr^{EYFP\Delta GHR}$ mice (Suppl. Figure 2).

3.2. Normal body weight in $Lepr^{EYFP\Delta GHR}$ -mice

To assess the impact of GHR deletion in LepRb neurons on energy balance, we compared body weight and body composition of control

and $Lepr^{EYFP\Delta GHR}$ male mice. $Lepr^{EYFP\Delta GHR}$ -mice displayed no alterations in body weight relative to controls between 4 and 24 weeks of age (Figure 3A), and both genotypes responded to high-fat diet (HFD) with similar increases in weight gain (Suppl. Figure 5A). Consistent with these findings, circulating serum leptin and adiponectin concentrations were indistinguishable between control and $Lepr^{EYFP\Delta GHR}$ male mice on chow diet and increased to the same extent on HFD (Figure 3D and Suppl. Figure. 3 and 5D). Similarly, fat and lean body mass on both chow and HFD were comparable between groups

A



B

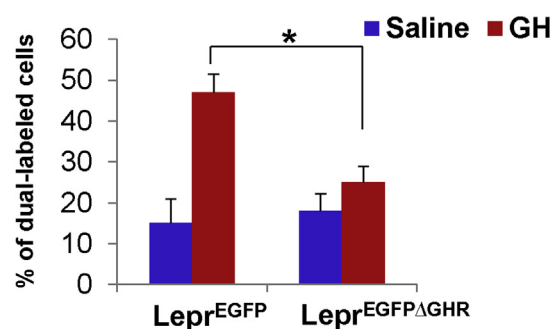


Figure 2: GHR signaling in $Lepr^{EYFP\Delta GHR}$ -mice. (A) Immunofluorescence for pStat5 in 6-month-old $Lepr^{EGFP}$ and $Lepr^{EYFP\Delta GHR}$ mice injected IP with vehicle (saline) or GH (12.5 $\mu\text{g}/100\text{ g BW}$; 1.5 h). Representative images from the ARH of $Lepr^{EGFP}$ and $Lepr^{EYFP\Delta GHR}$ mice are shown. Scale bar: 100 μm . The lower panels are digital zooms of boxed areas from the top panel, showing pStat5 (red) merged with EGFP (green) of the indicated genotypes (examples are shown by arrows). (B) Quantification of double labeled cells * $p < 0.05$. Quantification of LepRb/EGFP neurons containing pStat5 immunoreactivity ($n = 4/\text{genotype}$). Data are presented as mean \pm SEM; *, $p < 0.05$. See also Figure S2.

(Figure 3B, C and Suppl. Figure 5B, C). Furthermore, $Lepr^{EYFP\Delta GHR}$ mice showed food intake similar to control male mice (Figure 3E). Body length was indistinguishable between control and $Lepr^{EYFP\Delta GHR}$ mice, a further indication of the intact function of the growth pathway despite the absence of GHR signaling in LepRb neurons (data not shown). Body weight, serum levels of leptin, and GH and IGF1 concentrations were also unaltered in female mice (Suppl. Figure 4 and data not shown). Expression of anorexigenic neuropeptides (e.g., POMC) and orexigenic neuropeptides (such as NPY and AgRP) did not differ between

$Lepr^{EYFP\Delta GHR}$ mice and control male mice (Figure 3F). Taken together, these data indicate that energy homeostasis in mice is unaffected by selective, targeted disruption of the GHR gene in LepRb neurons.

3.3. $Lepr^{EYFP\Delta GHR}$ -mice exhibit impaired glucose homeostasis and fail to suppress hepatic glucose production

Next we investigated glucose homeostasis in $Lepr^{EYFP\Delta GHR}$ male mice. Basal blood glucose and serum insulin concentrations were indistinguishable between $Lepr^{EYFP\Delta GHR}$ mice as compared to controls

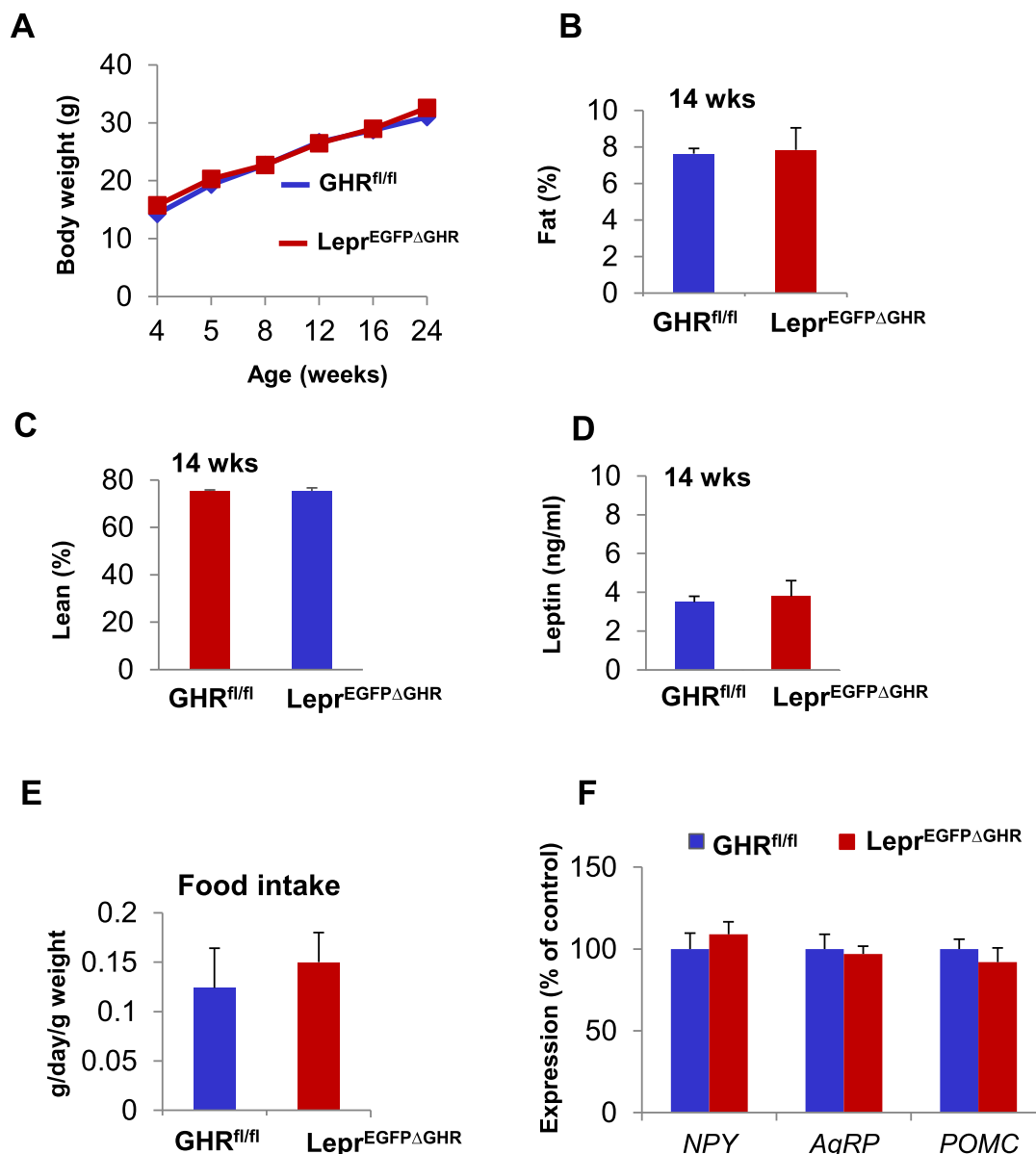


Figure 3: Normal body weight in *Lepr*^{EYFPΔGHR}-mice. (A) Average body weights of male *Lepr*^{EYFPΔGHR}-mice (red) and control *GHR*^{fl/fl}-mice (blue) on regular chow diet (n = 10). (B) Percent body fat and (C) lean body mass was determined by NMR using 14-week-old *GHR*^{fl/fl} (n = 5–6) and *Lepr*^{EYFPΔGHR} (n = 5–6) mice. (D) Serum leptin levels of 14-week-old male *GHR*^{fl/fl} (n = 8) and *Lepr*^{EYFPΔGHR} (n = 8) mice. (E) Food intake was measured for 6 consecutive days in 14-week-old male *GHR*^{fl/fl} (n = 8) and *Lepr*^{EYFPΔGHR} (n = 8) mice fed regular chow diet (F). Levels of mRNA by semi-quantitative RT-PCR of *NPY*, *AgRP*, and *POMC* from hypothalamus of 14-week-old chow-fed male mice of the indicated genotypes (n = 6). Data are presented as mean ± SEM. See also Figures. S1(B, C)–S5.

(Figure 4A–C). Despite normal fasting glucose levels, *Lepr*^{EYFPΔGHR} mice displayed significant glucose intolerance in response to an intraperitoneal glucose load on both chow and HFD (Figure 4A, D). Insulin tolerance was subsequently tested to determine whether this glucose intolerance was associated with systemic insulin resistance. However, the glucose-lowering effect of insulin and the rate of glucose disappearance (calculated as the slope from time 0 to 30) during the insulin tolerance test (ITT) were similar in both groups (Figure 4E, F). Insulin tolerance also did not differ between control and *Lepr*^{EYFPΔGHR} mice after 10 weeks on the HFD (data not shown). To assess the contribution of individual tissues to glucose metabolism, we performed a hyperinsulinemic-euglycemic clamp on *Lepr*^{EYFPΔGHR} and control

mice at 14–16 weeks of age. Clamp studies allow for an accurate determination of insulin-dependent peripheral glucose uptake and liver glucose output *in vivo* [27]. During the clamp, the glucose infusion rate required to maintain euglycemia was significantly reduced in *Lepr*^{EYFPΔGHR} compared to control mice ($p < 0.002$) (Figure 5A, B). Under basal conditions, whole-body glucose utilization, equivalent to endogenous hepatic glucose production (HGP), did not differ between control and *Lepr*^{EYFPΔGHR} mice (Figure 5C and Suppl. Figure 6). The major difference in glucose turnover rate between the groups came during clamp conditions when HGP was reduced to a greater extent in control (64%) vs. *Lepr*^{EYFPΔGHR} (25%) ($p < 0.005$) (Figure 5D). Steady-state serum insulin levels, whole body glucose clearance, and

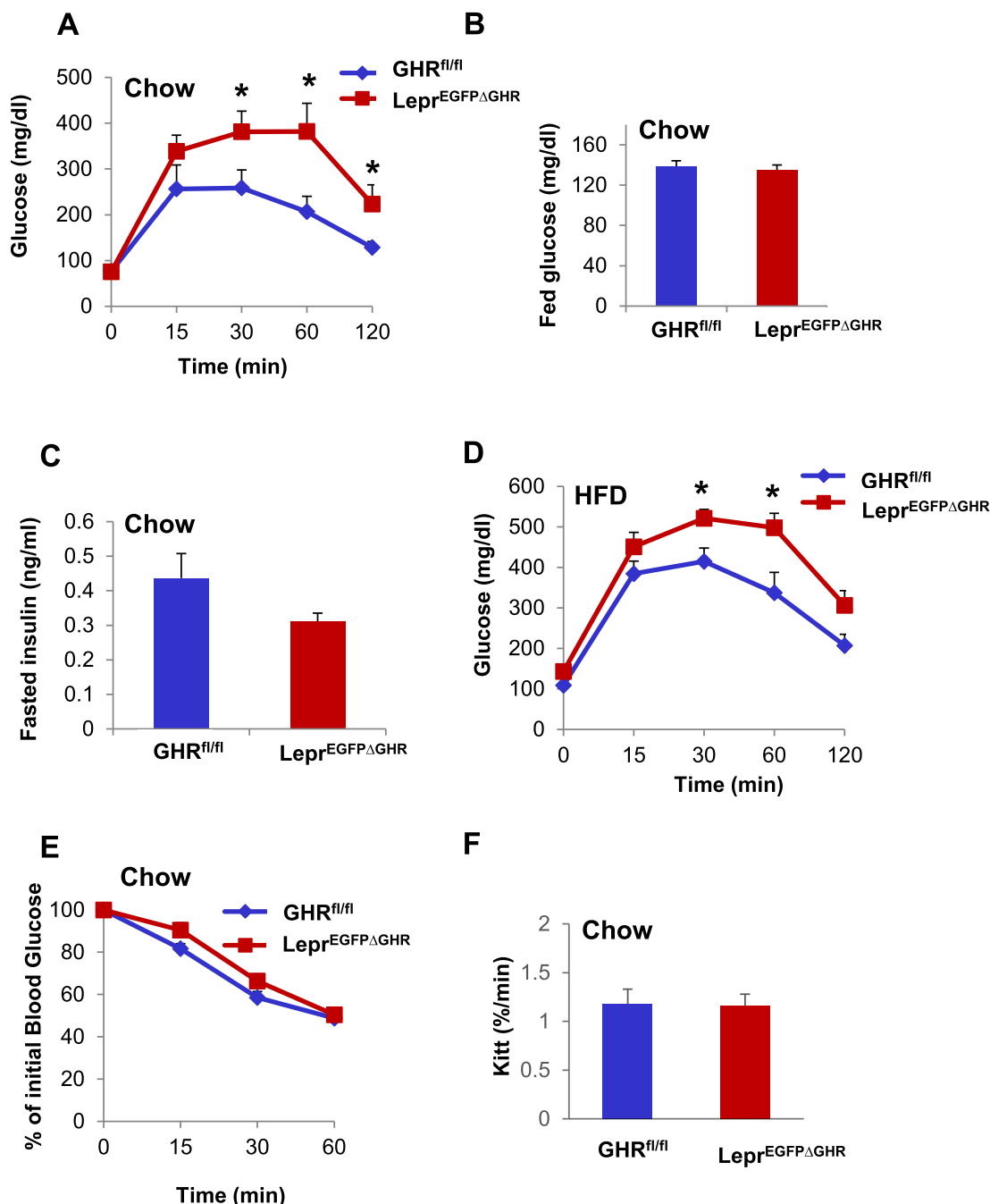


Figure 4: Glucose homeostasis in *Lepr^{EYFPΔGHR}* mice. (A) Glucose tolerance test of 16-week-old chow-fed male mice, (B) fed glucose levels ($n = 10$ /genotype) and (C) fasting serum insulin levels ($n = 10$ /genotype) for 16 week-old male mice of the indicated genotypes. (D) Glucose tolerance test of 24-week-old high-fat diet (HFD) fed mice of the indicated genotypes ($n = 5-6$ /genotype). (E) Insulin tolerance test of 17-week-old mice ($n = 8-10$ /genotype). (F) Serum glucose disappearance rate (Kitt, %/min) from the insulin tolerance test. Data are expressed as mean \pm SEM. GHR^{fl/fl} mice versus Lepr^{EYFPΔGHR} mice: *, $p < 0.05$. See also Figure S5.

glycolysis were indistinguishable between control and Lepr^{EYFPΔGHR} mice (Figure 5E and Suppl. Figure 6). Determination of tissue-specific glucose uptake rates showed similar rates of insulin-stimulated glucose uptake in skeletal muscle and adipose tissue in both groups of mice (Figure 5F). These data demonstrate that the observed whole-body glucose intolerance in Lepr^{EYFPΔGHR} mice is driven mainly by changes in hepatic gluconeogenesis rather than by changes in glucose uptake by peripheral tissue.

The levels of basal free fatty acids (FFAs) were not significantly different between control and Lepr^{EYFPΔGHR} mice (Figure 6A).

During the clamp, insulin-induced suppression of plasma FFA concentrations was less in Lepr^{EYFPΔGHR} mice (Figure 6A), suggesting an impairment in the ability of insulin to suppress lipolysis in these mice. Fasted triglyceride (TG) levels were not significantly different between the control (GHR^{fl/fl} 107.6 ± 21.2), and Lepr^{EYFPΔGHR} (86.9 ± 12.35 mg/dL) mice (Suppl. Figure 7A), and expression of *ACC1*, *FASN*, *SREBP-2* and *SREBP-1c* was unaltered (Suppl. Figure 7C). In contrast, fasted LDL levels were significantly increased in the Lepr^{EYFPΔGHR} vs. control mice (GHR^{fl/fl} $28.8.6 \pm 1.77$, and Lepr^{EYFPΔGHR} 41.02 ± 2.94 mg/dL) (Suppl. Figure 7B). Together

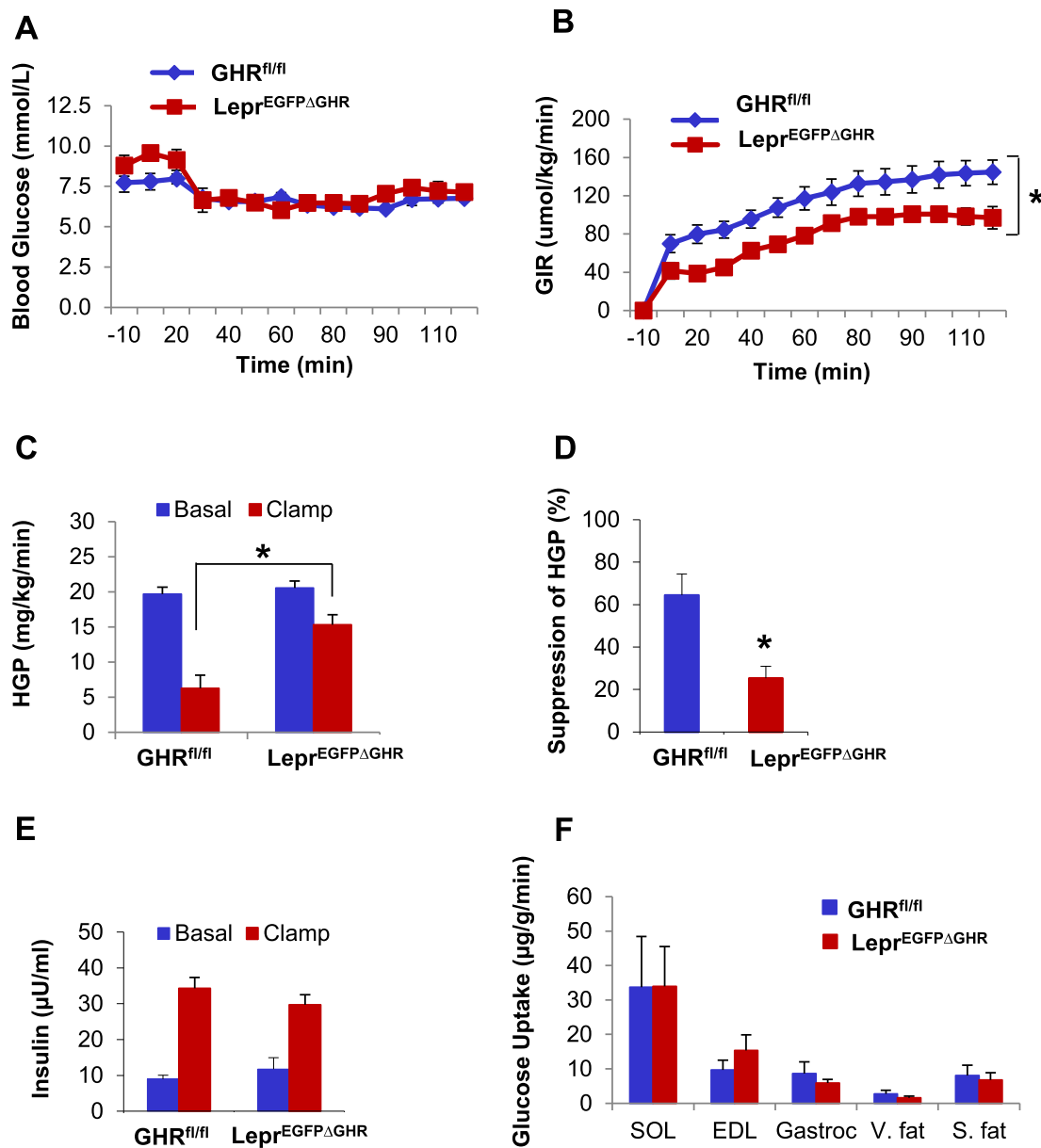


Figure 5: Hyperinsulinemic-euglycemic clamp in $Lepr^{EYFP\Delta GHR}$. (A) Blood glucose levels during the clamp period (B) Glucose infusion rates during the clamp period ($p < 0.002$). (C) Hepatic glucose production (HGP) measured under basal and steady-state conditions during the clamp ($p < 0.005$ for clamp). (D) Percentage suppression of HGP by insulin as measured under steady-state conditions during the clamp ($p < 0.005$). (E) Steady-state serum insulin levels. (F) Tissue-specific insulin-stimulated glucose uptake rates in skeletal muscle and adipose tissue (SOL, soleus muscle; EDL, extensor digitorum longus muscle; gastroc, gastrocnemius muscle; V. Fat, visceral fat; S. Fat, subcutaneous fat), in control and $Lepr^{EYFP\Delta GHR}$ male mice at 14–16 weeks of age, $n = 6$ mice per group. See also [Figure S6](#).

these findings indicate that loss of GHR in $LepR$ -b neurons affects central regulation of HGP and also influences peripheral lipid metabolism.

To determine whether insulin regulation of hepatic expression of key gluconeogenic genes was intact, real-time PCR was performed in livers from fasted animals and following the hyperinsulinemic-euglycemic clamp. Clamp steady-state expression of the glucose-6-phosphatase protein ($G6Pase$) and phosphoenolpyruvate carboxykinase 1 ($Pck1$) was significantly greater in liver of $Lepr^{EYFP\Delta GHR}$ mice than in control mice ($p < 0.05$) ([Figure 6B](#)). Prior to the hyperinsulinemic clamp procedure, the basal levels of $G6Pase$, and $Pck1$ were comparable in both groups (data not shown).

3.4. Hepatic signaling in $Lepr^{EYFP\Delta GHR}$ -mice

To explore the molecular basis for reduced hepatic insulin sensitivity, we next determined whether this effect was associated with impaired insulin signal transduction in the livers of $Lepr^{EYFP\Delta GHR}$ mice. To test this possibility, we examined the levels of phosphorylation of two key components in the insulin signaling pathways [34], insulin receptor substrate 1 (IRS-1) and protein kinase B (Akt), in liver after i.v. injection of insulin, as described previously [26]. As shown in [Figure 7A, B](#), insulin-stimulated phosphorylation of IRS-1 was significantly attenuated in the liver of $Lepr^{EYFP\Delta GHR}$ mice. Consistent with these results, insulin-stimulated Akt^{Ser473} phosphorylation was significantly reduced in the liver of $Lepr^{EYFP\Delta GHR}$ mice as compared with control mice

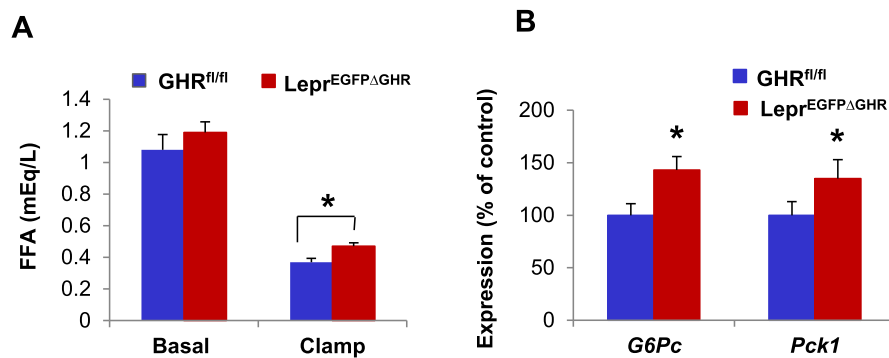


Figure 6: Levels of FFA and gluconeogenic genes under hyperinsulinemic clamp in Lepr^{EYFPΔGHR}-mice. (A) The levels of free fatty acids (FFAs) at the basal level and during the clamp in 14–16 weeks old control and Lepr^{EYFPΔGHR}-mice, n = 6 mice per group. (B) *G6Pc* and *Pck1* mRNA expression in liver at the end of hyperinsulinemic-euglycemic clamp in control and Lepr^{EYFPΔGHR} male mice at 14–16 weeks of age, n = 6 mice per group. Displayed values are means ± SEM, *, p < 0.05. See also Figure S7.

(p < 0.05) (Figure 7C), and further supports the induction of hepatic insulin resistance in this model.

4. DISCUSSION

We have generated a new mouse model to dissect the role of CNS GHR signaling in LepRb expressing neurons. Our results identify for

the first time a population of neurons responsible for the hypothalamic actions of GHR on hepatic glucose production (HGP). Specifically, loss of GHR in LepRb-expressing neurons of the ARH, DMH and LHA impairs the ability of insulin to regulate HGP and peripheral lipid metabolism. Importantly, these effects are mediated via mechanisms that are independent of hormonal changes or body adiposity.

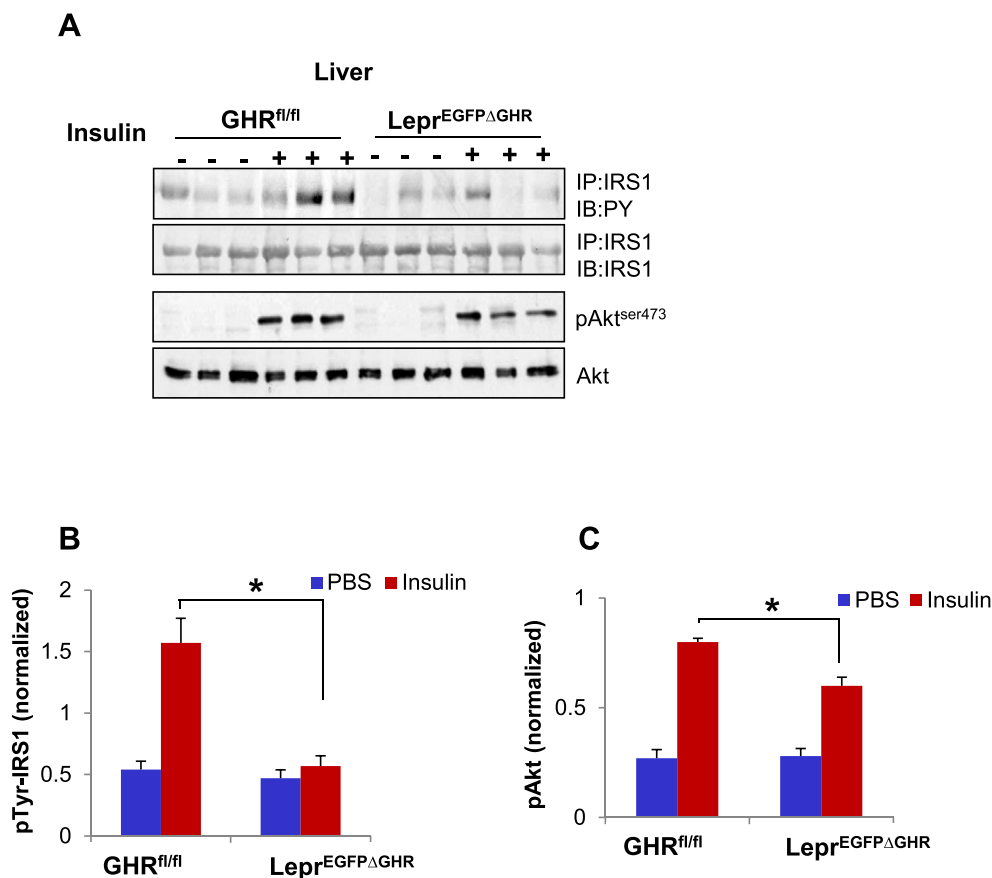


Figure 7: Hepatic Insulin Signaling in Lepr^{EYFPΔGHR}-mice. Mice in each experimental group were fasted overnight and stimulated with insulin (Ins) or PBS by i.v. injection (5 min). (A) Insulin receptor substrate 1 (IRS1) level and tyrosine phosphorylation in liver extracts. Akt and its phosphorylated form (phospho-Ser473) were analyzed with specific antibodies in the liver lysates. Quantification of (B) pTyr-IRS1 and (C) pAkt. Results were normalized to loading controls and are expressed as mean ± SEM, n = 6. *p < 0.05 for 14-week-old control vs Lepr^{EYFPΔGHR} male mice.

Recent analysis of the distribution of GH-responsive cells revealed the abundance of GH-responsive neurons in hypothalamic nuclei involved in the control of metabolism, such as the ARH, VMH, and DMH. This suggests that central GH signaling might be involved in energy expenditure and glucose homeostasis through a central mechanism [10]. GH overexpression in the CNS results in hyperphagia-induced obesity, insulin resistance, and increased circulating GH levels [17]. Additional studies reported obesity after expressing GH and GH-releasing hormone in the CNS, which has been attributed to lowering of endogenous GH levels [35,36]. However, these animal models did not dissect the effect of GH signaling in specifically defined neurons in the CNS, since they utilized CNS-wide promoters and had confounding effect of chronically altered GH levels. In contrast, we show that specific deletion of GHR signaling in LepRb neurons impairs insulin's ability to suppress hepatic glucose production independent of changes in IGF-1 or GH circulating levels. Moreover, LepRb neuron-restricted inactivation of the GHR does not interfere with the regulation of food intake or energy homeostasis under normal conditions or under high-fat diet, thus allowing determination of direct effects of central GHR signals on other tissues.

Decreases in glucose levels are detected by glucose-sensing neurons that are found in several brain regions including the VMH, the LHA, the ARH, as well as in several hindbrain regions [37,38]. GH release contributes to glucose counter-regulation by shifting metabolism of non-neural tissues away from glucose utilization [39]. Hypothalamic GH releasing hormone (GHRH) neurons are glucose responsive, increasing activity in response to decreasing glucose levels [40]. However, the direct actions of GH are mediated through GHR [5], and very few GHRH neurons express GHR [41]. LepRb neurons regulate glucose homeostasis, and our data show that they co-express GHR in the ARH, DMH, and LHA neurons. Lean $\text{Lepr}^{\text{EYFP}\Delta\text{GHR}}$ mice are not GH deficient but are hyperglycemic after a glucose load and have impaired HGP and lipid metabolism. Thus, one may speculate that the GHR in hypothalamic LepRb neuronal subsets of the ARH, DMH, and LHA directly or indirectly facilitates insulin signaling. Cell-type specific ablation of GHR will be necessary to unravel the functional significance of GHR expressing neurons in controlling glucose metabolism independently of body weight.

Hepatic gluconeogenesis is a major contributing factor to hyperglycemia [42], and GH is reported to enhance hepatic gluconeogenesis [43]. This mechanism cannot explain impaired HGP in $\text{Lepr}^{\text{EYFP}\Delta\text{GHR}}$ mice, since they have normal GH and IGF-1 levels. Consistent with the marked increase of HGP, insulin-induced suppression of hepatic gluconeogenic genes *G6Pase* and *Pck1* expression is blunted and hepatic insulin signaling reduced, indicating that increased hepatic gluconeogenesis and impaired insulin signaling contributed to hyperglycemia provoked by deleting GHR from specific LepRb neuronal subsets. We cannot, however, rule out the possibility that reduced hepatic insulin signaling is a secondary effect [44], since $\text{Lepr}^{\text{EYFP}\Delta\text{GHR}}$ mice are not insulin resistant. The ability of insulin to decrease plasma fatty acid concentrations during the hyperinsulinemic-euglycemic clamp was also reduced in $\text{Lepr}^{\text{EYFP}\Delta\text{GHR}}$ mice, suggesting that insulin suppression of lipolysis was impaired, which might contribute to hepatic insulin resistance through direct or indirect generation of metabolites that alter the insulin-signaling cascade [45]. Increased plasma total cholesterol levels in $\text{Lepr}^{\text{EYFP}\Delta\text{GHR}}$ mice also can be attributed to increased cholesterol uptake and export from the liver. Further studies will be necessary to determine the effects of GHR-LepRb neuronal subsets on lipid metabolism and the interaction with other hormones that regulate HGP.

HGP can be stimulated by increased activity of the sympathetic input to the liver or decreased activity of the parasympathetic input to the liver

[46,47]. The parasympathetic tone in rats might be physiologically relevant in controlling the basal HGP [48]. Vagus nerve innervation is important in mediating brain insulin control of hepatic glucose homeostasis [49]. Proper functioning of the vagus nerve is important for production of GHRH and IGF-1 [50]. It is reasonable to hypothesize that vagus nerve innervations are involved in central GHR signaling effect on glucose metabolism. The sympathetic nervous system (SNS) has been implicated in leptin actions [51], and in central insulin mediated lipogenesis [52]. Additional studies will be necessary to delineate the role of the two branches of the autonomic nervous system in the central GHR-mediated HGP.

It has been shown previously that hypothalamic leptin and insulin signaling are required for the inhibition of HGP [53–56]. Indeed, intracerebroventricular infusion of insulin or leptin in rodents can potentially suppress hepatic glucose production, whereas antagonism of insulin or leptin signaling in the hypothalamus can impair the ability of peripheral insulin to suppress HGP [55,56]. Evidence suggests that NPY neurons are involved in this process [57]. Interestingly, increased CNS NPY signaling can modulate hepatic lipoprotein metabolism [58]. The majority of neuropeptide Y (NPY) neurons in the ARH co-express GHR and LepRb [59], and NPY neurons mediate the feedback effect of GH on the hypothalamus [13]. The functional significance of GH signals on NPY neurons remains somewhat undefined [60]. Thus it is possible to speculate that NPY- LepRb neuronal circuitry is involved in the physiology of GHR responses, and might regulate its function.

Previous studies indicate that LepRb-DMH neurons strongly connect to the PVH [61], and PVH regulates glucose homeostasis, probably via the sympathetic nervous system (SNS)-liver axis [62], thus suggesting a role for the DMH in glucose metabolism. Conversely, while it is unlikely that LepRb-LHA neurons mediate leptin's anti-diabetic actions in the regulation of glucose homeostasis [63,64], it can still be speculated that LepRb-LHA neurons provide an essential output for autonomic responses, since a significant subpopulation of LHA neurons are glucose inhibited [65], and their role in GH responses or GHR signaling is unclear. Future identification of these GHR-LepRb neuronal subsets will be required to understand how these are controlled differentially and to determine the respective roles of these neuronal populations and their hypothalamic circuitry in the control of glucose metabolism. Leptin signaling may be important in the maintenance of somatotropes, acting directly at the level of the pituitary [66]. Interestingly, somatotrope-specific *Lepr* knockouts showed reduced serum GH and increased fat mass and impaired Stat3 signaling, demonstrating the importance of leptin in the direct regulation of somatotrope function [67]. We and others did not detect expression of *Lepr-cre* in pituitary (data not shown), and the expression of GHR in the pituitaries of $\text{Lepr}^{\text{EYFP}\Delta\text{GHR}}$ mice was intact. Furthermore, deletion of GHR from LepRb neurons had no effect on Stat3 signaling or serum GH levels. In support of this idea, growth and adiposity of $\text{Lepr}^{\text{EYFP}\Delta\text{GHR}}$ mice were normal.

GH secretion is consistently reduced in obesity [68]. The hyperinsulinemia associated with insulin resistance in obesity has been suggested to contribute to reduced GH secretion [32]. Obesity-induced leptin resistance and increased bioactive IGF-1 and FFA levels could suppress GH secretion from the pituitary by various mechanisms [41]. HFD fed $\text{Lepr}^{\text{EYFP}\Delta\text{GHR}}$ mice showed significantly higher glucose levels in response to an intraperitoneal glucose load as compared to control glucose intolerant mice. This data suggests that deletion of central GHR signaling in LepRb neurons might exacerbate the GH-resistant state that is associated with obesity and contribute to diet-induced obesity complications. In support, a recent study demonstrated that chronic,

peripheral GH injections significantly improved glucose metabolism and reduced liver triacylglycerol content of normal HFD fed mice, suggesting an effectiveness of GH therapy in the treatment of diet-induced obesity [69].

The activation of GHR induces Stat5 phosphorylation [33], and cells that exhibit pStat5-immunoreactivity after an acute GH stimulation are considered to be GH responsive [10]. A previous study demonstrated strong GH-induced pStat5 immunoreactive cells in the ARH, VMH, PVH, and some additional hypothalamic and extra hypothalamic areas [10,70]. We detected very low GH-induced pStat5-IR cells among LepRb neurons in the LepR^{EYFPΔGHR} mice compared to controls, indicating that GH signaling is impaired. Hypothalamic Stat5 can mediate the direct negative feedback effects by GH [71]. Neuronal deletion of Stat5 results in obesity, insulin resistance, and glucose intolerance [72]. LepRb specific Stat5 KO mice have normal body weight regulation [73]; however, no data on the regulation of glucose metabolism was reported. Our data suggest that in specific neuronal populations, Stat5 signaling might be involved in GHR-mediated glucose homeostasis through a central mechanism.

Overall, our findings define the physiological role of GHR signaling in distinct LepRb-expressing neuronal populations. We find no role for GHR in LepRb neurons in the regulation of food intake or body weight, but our data provide powerful genetic evidence for a direct role of central GHR signals in LepRb neurons in the regulation of glucose homeostasis and hepatic glucose production. GH treatment in obese type 2 diabetes patients decreases amounts of fat and improves insulin resistance [74]. We have identified LepRb-GHR neuronal populations as a crucial factor for the anti-diabetic actions of GH signaling. Understanding the molecular mechanisms operating in these neurons will yield new targets for treating obesity-driven metabolic diseases. Further identification, manipulation, and understanding of the function of specific GHR neuronal populations will be critical to address the physiological relevance of these findings for the development of metabolic diseases.

AUTHOR CONTRIBUTIONS

GC carried out the research and reviewed the manuscript. TL and MG performed research. JJK and MGM provided animal models and reviewed and revised the manuscript. NQ designed studies related to hyperinsulinemic-euglycemic clamp, carried out this aspect of the research, and interpreted the results. DAS and CE designed parts of the study, interpreted the results, and reviewed and revised the manuscript. RAM assisted in study design, provided animal models, and reviewed and revised the manuscript. MS designed the study, carried out the research, analyzed the data, wrote the manuscript, and is responsible for the integrity of this work. All authors approved the final version of the manuscript.

ACKNOWLEDGEMENTS

The authors thank Amanda Keedle, Sabrina Van Roekel, Natalie Perry and Roxann Alonzo for husbandry assistance, and Jessica Peck for technical assistance.

We acknowledge support from the National Institutes of Health (AG022303 for RAM and the Glenn Foundation for Medical Research for RAM, R01DH69702 for CE, DK056731 for MGM, DK082480 for DAS, JJK was supported by the State of Ohio's Eminent Scholar Program which includes a gift by Milton and Lawrence Goll. MS was supported by a pilot grant from the UM Pepper Center AG-024824, and a Feasibility Grant from the Michigan Diabetes Research Center (P30DK020572). This work utilized Core Services supported by grants DK089503 (MNORC) and DK020572 (MDRC) of NIH to the University of Michigan.

COMPETING FINANCIAL INTERESTS

DAS also receives research support from Ethicon Endo-Surgery Inc., Sanofi, and Novo Nordisk A/S.

APPENDIX A. SUPPLEMENTARY DATA

Supplementary data related to this article can be found at <http://dx.doi.org/10.1016/j.molmet.2017.03.001>.

CONFLICT OF INTEREST

DAS also receives research support from Ethicon Endo-Surgery Inc., Sanofi, and Novo Nordisk A/S.

REFERENCES

- [1] Bartke, A., 2011. Growth hormone, insulin and aging: the benefits of endocrine defects. *Experimental Gerontology* 46(2–3):108–111.
- [2] Moller, N., Jorgensen, J.O., 2009. Effects of growth hormone on glucose, lipid, and protein metabolism in human subjects. *Endocrine Reviews* 30(2):152–177.
- [3] Bartke, A., Sun, L.Y., Longo, V., 2013. Somatotrophic signaling: trade-offs between growth, reproductive development, and longevity. *Physiological Review* 93(2):571–598.
- [4] Alessi, D.R., 2001. Discovery of PDK1, one of the missing links in insulin signal transduction. Colworth Medal Lecture. *Biochemical Society Transactions* 29(Pt 2):1–14.
- [5] Ahn, C.W., et al., 2006. Effects of growth hormone on insulin resistance and atherosclerotic risk factors in obese type 2 diabetic patients with poor glycaemic control. *Clinical Endocrinology (Oxf)* 64(4):444–449.
- [6] Hojvat, S., et al., 1982. Growth hormone (GH) immunoreactivity in the rodent and primate CNS: distribution, characterization and presence post-hypophysectomy. *Brain Research* 239(2):543–557.
- [7] Kastrop, Y., et al., 2005. Distribution of growth hormone receptor mRNA in the brain stem and spinal cord of the rat. *Neuroscience* 130(2):419–425.
- [8] Lobie, P.E., et al., 1993. Localization and ontogeny of growth hormone receptor gene expression in the central nervous system. *Developmental Brain Research* 74(2):225–233.
- [9] Barzilai, N., Rossetti, L., 1993. Role of glucokinase and glucose-6-phosphatase in the acute and chronic regulation of hepatic glucose fluxes by insulin. *The Journal of Biological Chemistry* 268:25019–25025.
- [10] Furigo, I.C., et al., 2017. Distribution of growth hormone-responsive cells in the mouse brain. *Brain Structure & Function* 222(1):341–363.
- [11] Moutoussamy, S., Kelly, P.A., Finidori, J., 1998. Growth-hormone-receptor and cytokine-receptor-family signaling. *European Journal Biochemistry* 255(1):1–11.
- [12] Herrington, J., Carter-Su, C., 2001. Signaling pathways activated by the growth hormone receptor. *Trends in Endocrinology Metabolism: TEM* 12(6):252–257.
- [13] Kamegai, J., et al., 1996. Growth hormone receptor gene is expressed in neuropeptide Y neurons in hypothalamic arcuate nucleus of rats. *Endocrinology* 137(5):2109–2112.
- [14] Wallenius, K., et al., 2001. Liver-derived IGF-I regulates GH secretion at the pituitary level in mice. *Endocrinology* 142(11):4762–4770.
- [15] List, E.O., et al., 2011. Endocrine parameters and phenotypes of the growth hormone receptor gene disrupted (GHR^{-/-}) mouse. *Endocrine Review* 32(3): 356–386.
- [16] Flurkey, K., et al., 2001. Lifespan extension and delayed immune and collagen aging in mutant mice with defects in growth hormone production. *Proceedings of the National Academy Sciences of United States of America* 98(12):6736–6741.
- [17] Bohlooly, Y.M., et al., 2005. Growth hormone overexpression in the central nervous system results in hyperphagia-induced obesity associated with insulin resistance and dyslipidemia. *Diabetes* 54(1):51–62.

- [18] Gahete, M.D., et al., 2011. Elevated GH/IGF-I, due to somatotrope-specific loss of both IGF-I and insulin receptors, alters glucose homeostasis and insulin sensitivity in a diet-dependent manner. *Endocrinology* 152(12):4825–4837.
- [19] Sadagurski, M., et al., 2015. Growth hormone modulates hypothalamic inflammation in long-lived pituitary dwarf mice. *Aging Cell* 14(6):1045–1054.
- [20] Sonntag, W.E., et al., 2013. Insulin-like growth factor-1 in CNS and cerebrovascular aging. *Frontiers in Aging Neuroscience* 5:27.
- [21] Leshan, R.L., et al., 2006. Leptin receptor signaling and action in the central nervous system. *Obesity (Silver Spring)* 14(Suppl 5):208S–212S.
- [22] Watanobe, H., Habu, S., 2002. Leptin regulates growth hormone-releasing factor, somatostatin, and alpha-melanocyte-stimulating hormone but not neuropeptide Y release in rat hypothalamus in vivo: relation with growth hormone secretion. *The Journal of Neuroscience* 22(14):6265–6271.
- [23] Costanzo, M., et al., 2010. The genetic landscape of a cell. *Science* 327(5964):425–431.
- [24] Allison, M.B., et al., 2015. TRAP-seq defines markers for novel populations of hypothalamic and brainstem LepRb neurons. *Molecular Metabolism* 4(4):299–309.
- [25] List, E.O., et al., 2014. Liver-specific GH receptor gene-disrupted (LiGHRKO) mice have decreased endocrine IGF-I, increased local IGF-I, and altered body size, body composition, and adipokine profiles. *Endocrinology* 155(5):1793–1805.
- [26] Sadagurski, M., et al., 2010. Human IL6 enhances leptin action in mice. *Diabetologia* 53(3):525–535.
- [27] Ayala, J.E., et al., 2011. Hyperinsulinemic-euglycemic clamps in conscious, unrestrained mice. *Journal of Visualized Experiments*(57).
- [28] Carew, R.M., et al., 2010. Deletion of *Irs2* causes reduced kidney size in mice: role for inhibition of GSK3beta? *BMC Developmental Biology* 10:73.
- [29] Patterson, C.M., et al., 2010. Large litter rearing enhances leptin sensitivity and protects selectively bred diet-induced obese rats from becoming obese. *Endocrinology* 151(9):4270–4279.
- [30] Cravo, R.M., et al., 2011. Characterization of Kiss1 neurons using transgenic mouse models. *Neuroscience* 173:37–56.
- [31] Zigman, J.M., et al., 2006. Expression of ghrelin receptor mRNA in the rat and the mouse brain. *The Journal of Comparative Neurology* 494(3):528–548.
- [32] Berryman, D.E., et al., 2013. The GH/IGF-1 axis in obesity: pathophysiology and therapeutic considerations. *Nature Review Endocrinology* 9(6):346–356.
- [33] Ihle, J.N., 1996. STATs: signal transducers and activators of transcription. *Cell* 84:331–334.
- [34] Lee, Y.H., White, M.F., 2004. Insulin receptor substrate proteins and diabetes. *Archives Pharmacol Research* 27(4):361–370.
- [35] Ikeda, A., et al., 1998. Obesity and insulin resistance in human growth hormone transgenic rats. *Endocrinology* 139(7):3057–3063.
- [36] Cai, A., Hyde, J.F., 1999. The human growth hormone-releasing hormone transgenic mouse as a model of modest obesity: differential changes in leptin receptor (OBR) gene expression in the anterior pituitary and hypothalamus after fasting and OBR localization in somatotrophs. *Endocrinology* 140(8):3609–3614.
- [37] Borg, W.P., et al., 1995. Local ventromedial hypothalamus glucopenia triggers counterregulatory hormone release. *Diabetes* 44(2):180–184.
- [38] Schwartz, N.S., et al., 1987. Glycemic thresholds for activation of glucose counterregulatory systems are higher than the threshold for symptoms. *Journal of Clinical Investigation* 79(3):777–781.
- [39] Stanley, S., et al., 2013. Profiling of glucose-sensing neurons reveals that GHRH neurons are activated by hypoglycemia. *Cell Metabolism* 18(4):596–607.
- [40] Chan, Y.Y., Steiner, R.A., Clifton, D.K., 1996. Regulation of hypothalamic neuropeptide-Y neurons by growth hormone in the rat. *Endocrinology* 137(4):1319–1325.
- [41] Vijayakumar, A., Yakar, S., Leroith, D., 2011. The intricate role of growth hormone in metabolism. *Frontiers in Endocrinology (Lausanne)* 2:32.
- [42] Pilkis, S.J., El-Maghrabi, M.R., 1988. Hormonal regulation of hepatic gluconeogenesis and glycolysis. *Annual Review of Biochemistry* 57:755–783.
- [43] Vijayakumar, A., et al., 2010. Biological effects of growth hormone on carbohydrate and lipid metabolism. *Growth Hormone & IGF Research* 20(1):1–7.
- [44] Titchenell, P.M., et al., 2015. Hepatic insulin signalling is dispensable for suppression of glucose output by insulin in vivo. *Nature Communication* 6:7078.
- [45] Delarue, J., Magnan, C., 2007. Free fatty acids and insulin resistance. *Current Opinion in Clinical Nutrition Metabolic Care* 10(2):142–148.
- [46] Shimazu, T., 1967. Glycogen synthetase activity in liver: regulation by the autonomic nerves. *Science* 156(3779):1256–1257.
- [47] Nonogaki, K., 2000. New insights into sympathetic regulation of glucose and fat metabolism. *Diabetologia* 43(5):533–549.
- [48] Matsuhiwa, M., et al., 2000. Important role of the hepatic vagus nerve in glucose uptake and production by the liver. *Metabolism* 49(1):11–16.
- [49] Rojas, J.M., Schwartz, M.W., 2014. Control of hepatic glucose metabolism by islet and brain. *Diabetes Obesity & Metabolism* 16(Suppl 1):33–40.
- [50] Al-Massadi, O., et al., 2011. The vagus nerve as a regulator of growth hormone secretion. *Regulatory Peptides* 166(1–3):3–8.
- [51] Rahmouni, K., 2010. Leptin-induced sympathetic nerve activation: signaling mechanisms and cardiovascular consequences in obesity. *Current Hypertension Reviews* 6(2):104–209.
- [52] Scherer, T., et al., 2011. Brain insulin controls adipose tissue lipolysis and lipogenesis. *Cell Metabolism* 13(2):183–194.
- [53] Koch, L., et al., 2008. Central insulin action regulates peripheral glucose and fat metabolism in mice. *The Journal of Clinical Investigation* 118(6):2132–2147.
- [54] Poci, A., et al., 2005. A brain-liver circuit regulates glucose homeostasis. *Cell Metabolism* 1(1):53–61.
- [55] Obici, S., et al., 2002. Hypothalamic insulin signaling is required for inhibition of glucose production. *Nature Medicine* 8(12):1376–1382.
- [56] Poci, A., et al., 2005. Central leptin acutely reverses diet-induced hepatic insulin resistance. *Diabetes* 54(11):3182–3189.
- [57] Konner, A.C., et al., 2007. Insulin action in AgRP-expressing neurons is required for suppression of hepatic glucose production. *Cell Metabolism* 5(6):438–449.
- [58] Stafford, J.M., et al., 2008. Central nervous system neuropeptide Y signaling modulates VLDL triglyceride secretion. *Diabetes* 57(6):1482–1490.
- [59] Adams, J., Collaco-Moraes, Y., de Belleruche, J., 1996. Cyclooxygenase-2 induction in cerebral cortex: an intracellular response to synaptic excitation. *Journal of Neurochemistry* 66(1):6–13.
- [60] Steyn, F.J., 2015. Nutrient sensing overrides somatostatin and growth hormone-releasing hormone to control pulsatile growth hormone release. *Journal of Endocrinology* 27(7):577–587.
- [61] Gautron, L., et al., 2010. Identifying the efferent projections of leptin-responsive neurons in the dorsomedial hypothalamus using a novel conditional tracing approach. *The Journal of Comparative Neurology* 518(11):2090–2108.
- [62] Collombat, P., et al., 2009. The ectopic expression of Pax4 in the mouse pancreas converts progenitor cells into alpha and subsequently beta cells. *Cell* 138(3):449–462.
- [63] Leininger, G.M., 2009. Location, location, location: the CNS sites of leptin action dictate its regulation of homeostatic and hedonic pathways. *International Journal of Obesity (Lond)* 33(Suppl 2):S14–S17.
- [64] Leininger, G.M., et al., 2011. Leptin action via neurotensin neurons controls orexin, the mesolimbic dopamine system and energy balance. *Cell Metabolism* 14(3):313–323.
- [65] Marston, O.J., et al., 2011. Neuropeptide Y cells represent a distinct glucose-sensing population in the lateral hypothalamus. *Endocrinology* 152(11):4046–4052.
- [66] Popovic, V., et al., 2001. Leptin and the pituitary. *Pituitary* 4(1–2):7–14.
- [67] Akhter, N., et al., 2012. Ablation of leptin signaling to somatotropes: changes in metabolic factors that cause obesity. *Endocrinology* 153(10):4705–4715.
- [68] Snyder, D.K., Clemmons, D.R., Underwood, L.E., 1988. Treatment of obese, diet-restricted subjects with growth hormone for 11 weeks: effects on

- anabolism, lipolysis, and body composition. *The Journal of Clinical Endocrinology and Metabolism* 67(1):54–61.
- [69] List, E.O., et al., 2009. Growth hormone improves body composition, fasting blood glucose, glucose tolerance and liver triacylglycerol in a mouse model of diet-induced obesity and type 2 diabetes. *Diabetologia* 52(8):1647–1655.
- [70] Bennett, E., et al., 2005. Hypothalamic STAT proteins: regulation of somatostatin neurones by growth hormone via STAT5b. *Journal of Neuroendocrinology* 17(3):186–194.
- [71] Flores-Morales, A., et al., 2006. Negative regulation of growth hormone receptor signaling. *Molecular Endocrinology* 20(2):241–253.
- [72] Abbas, A., Grant, P.J., Kearney, M.T., 2008. Role of IGF-1 in glucose regulation and cardiovascular disease. *Expert Review of Cardiovascular Therapy* 6(8): 1135–1149.
- [73] Singireddy, A.V., et al., 2013. Neither signal transducer and activator of transcription 3 (STAT3) or STAT5 signaling pathways are required for leptin's effects on fertility in mice. *Endocrinology* 154(7):2434–2445.
- [74] Nam, S.Y., et al., 2001. Low-dose growth hormone treatment combined with diet restriction decreases insulin resistance by reducing visceral fat and increasing muscle mass in obese type 2 diabetic patients. *International Journal of Obesity and Related Metabolism Disorders* 25(8):1101–1107.